ARTICLE

Microparticles enhance the formation of seven major classes of natural products in native and metabolically engineered actinobacteria through accelerated morphological development

Martin Kuhl[1] | Christian Rückert[3] | Lars Gläser[1] | Selma Beganovic[1] | Andriy Luzhetskyy[2] | Jörn Kalinowski[3] | Christoph Wittmann[1] (ORCID)

[1]Institute of Systems Biotechnology, Saarland University, Saarbrücken, Germany

[2]Department of Pharmaceutical Biotechnology, Saarland University, Saarbrücken, Germany

[3]Center for Biotechnology, Bielefeld University, Bielefeld, Germany

Correspondence
Christoph Wittmann, Institute of Systems Biotechnology, Saarland University, Saarbrücken, Germany.
Email: christoph.wittmann@uni-saarland.de

Abstract

Actinobacteria provide a rich spectrum of bioactive natural products and therefore display an invaluable source towards commercially valuable pharmaceuticals and agrochemicals. Here, we studied the use of inorganic talc microparticles (hydrous magnesium silicate, $3MgO \cdot 4SiO_2 \cdot H_2O$, 10 μm) as a general supplement to enhance natural product formation in this important class of bacteria. Added to cultures of recombinant *Streptomyces lividans*, talc enhanced production of the macrocyclic peptide antibiotic bottromycin A2 and its methylated derivative Met-bottromycin A2 up to 109 mg L^{-1}, the highest titer reported so far. Hereby, the microparticles fundamentally affected metabolism. With 10 g L^{-1} talc, *S. lividans* grew to 40% smaller pellets and, using RNA sequencing, revealed accelerated morphogenesis and aging, indicated by early upregulation of developmental regulator genes such as *ssgA*, *ssgB*, *wblA*, *sigN*, and *bldN*. Furthermore, the microparticles re-balanced the expression of individual bottromycin cluster genes, resulting in a higher macro-cyclization efficiency at the level of BotAH and correspondingly lower levels of non-cyclized shunt by-products, driving the production of mature bottromycin. Testing a variety of *Streptomyces* species, talc addition resulted in up to 13-fold higher titers for the RiPPs bottromycin and cinnamycin, the alkaloid undecylprodigiosin, the polyketide pamamycin, the tetracycline-type oxytetracycline, and the anthramycin-analogs usabamycins. Moreover, talc addition boosted production in other actinobacteria, outside of the genus of *Streptomyces*: vancomycin (*Amycolatopsis japonicum* DSM 44213), teicoplanin (*Actinoplanes teichomyceticus* ATCC 31121), and the angucyclinone-type antibiotic simocyclinone (*Kitasatospora* sp.). For teicoplanin, the microparticles were even crucial to activate production. Taken together, the use of talc was beneficial in 75% of all tested cases and optimized natural and hetero-logous hosts forming the substance of interest with clusters under native and

synthetic control. Given its simplicity and broad benefits, microparticle-supplementation appears as an enabling technology in natural product research of these most important microbes.

1 | INTRODUCTION

Natural products are chemically diverse molecules that are synthetized by living organisms (Harvey, 2000). Many of them have potent pharmacological activities, which has enabled the development of antibiotics (Fleming, 2001), anticancer drugs (Arcamone et al., 1969), immunosuppressants (Vézina et al., 1975), infectants (Campbell et al., 1983), and various agrochemicals, including herbicides (Bayer et al., 1972), insecticides (Butterworth & Morgan, 1968), and fungicides (Takeuchi et al., 1958). During the last century, natural products and their derivatives have greatly helped to double human life expectation (Demain, 2006) and display more than 50% of today's approved drugs (Cragg & Newman, 2013). However, drug development from natural products is declining, partly caused by unreliable access and supply, leading inter alia to cost and profit concerns among pharmaceutical companies (Li & Vederas, 2009).

Actinobacteria display the most important microbial source of natural products and therefore offer an immense treasure (Barka et al., 2016). The genus *Streptomyces* provides more than two-third of all known antibiotics of microbial origin (Bibb, 2013) and more than half of the FDA-approved antibacterial natural products (Patridge et al., 2015) but also related actinobacteria such as *Micromonospora*, *Actinoplanes*, and *Amycolatopsis* (Barka et al., 2016) have emerged as producers of potent bioactive molecules. Unfortunately, actinobacteria produce natural products often in minute amounts, making even structural identification almost impossible, or do not form them at all under laboratory conditions (Ren et al., 2017). Moreover, natural products exhibit complex, highly diverse biosynthetic pathways and structures (Figure 1), which complicates efforts to streamline and enhance production (Hanson, 2003). Towards optimized supply, general strategies that allow to enhance natural product formation in actinobacteria are highly desired.

At this point, a promising line of research seems to exploit the link between natural product formation and the unique morphological life cycle of actinobacteria (Chater, 1984), which differentiates them from most other bacteria (Barka et al., 2016). In liquid culture, their morphological development starts from germinated spores that grow into a vegetative mycelium by linear tip extension and hyphae branching (Chater & Losick, 1997; van Dissel et al., 2014), followed by the formation of an aerial mycelium, which finally differentiates into uninucleoid cells that develop again into spores (Angert, 2005). Recently, we discovered that supplementation with inorganic talc microparticles (hydrous magnesium silicate, $3MgO \cdot 4SiO_2 \cdot H_2O$)

reprogrammed recombinant *Streptomyces albus* J1074/R2 to live a life of accelerated morphogenesis, which enabled a three-fold enhanced production of the antituberculosis polyketide pamamycin (Kuhl et al., 2020).

Here, we took this approach further. Exemplified for recombinant *Streptomyces lividans* TK24 DG2-Km-P41hyg + (Horbal et al., 2018), the effects of talc were elucidated using transcriptomics and metabolomics together with detailed analysis of strain physiology and morphology. The recombinant producer, representing one of the most prestigious *Streptomyces* species used industrially (Sevillano et al., 2016), formed the ribosomally and posttranslationally modified peptide (RiPP) bottromycin under control of synthetic promoters, supposed to uncouple production from the morphological cell cycle. It displayed the leading cell factory to produce bottromycin (Vior et al., 2020). The cyclopeptide was first isolated from cultures of *Streptomyces bottropensis* (Waisvisz et al., 1957) and is active against methicillin-resistant *Staphylococcus aureus* and vancomycin-resistant *Enterococci* (Kobayashi et al., 2010). Its complex biosynthesis involves a unique posttranslational macrocyclization step (Huo et al., 2012) and has posed enormous challenges on bottromycin research and development over the past decades (Kazmaier, 2020).

Finally, the microparticle approach was scaled down to the microtiter plate scale to investigate its potential in overproducing twelve natural compounds of commercial interest from ten major structural classes in native and metabolically engineered actinobacteria, including various *Streptomyces* but also other genera and families (Figure 1).

2 | MATERIALS AND METHODS

2.1 | Strains

All strains used in this study are listed in Table 1. For strain maintenance, spores were collected from agar plate cultures after five-day incubation at 30°C, resuspended in 20% glycerol, and kept at −80°C.

2.2 | Media

Mannitol-soy flour agar was used for plate cultures of all strains. It contained per liter: 20 g mannitol (Sigma-Aldrich), 20 g soy flour (Schoenenberger Hensel), and 20 g agar (Becton & Dickinson). For
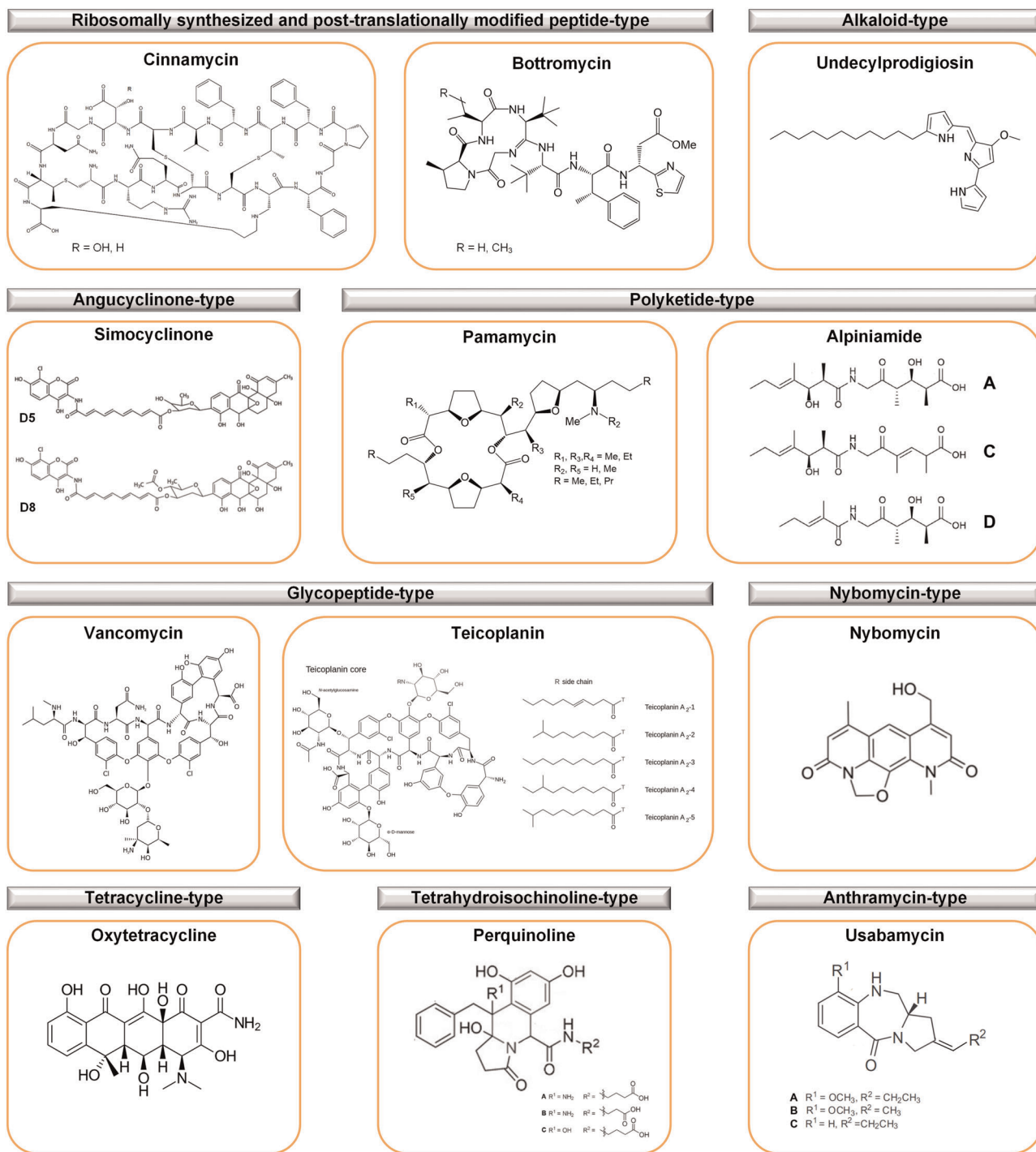
FIGURE 1 Natural products and their derivatives investigated in this study. The compounds comprise nine different chemical classes and have been previously described in different actinobacteria: *Streptomyces albus* pCinCatInt (cinnamycins) (Lopatniuk et al., 2017), *Streptomyces lividans* TK24 DG2-Km-P41hyg + (bottromycins) (Horbal et al., 2018), *Streptomyces lividans* TK24 (undecylprodigiosin) (Horinouchi & Beppu, 1984), *Kitasatospora* sp. (simocyclinones) (Bilyk et al., 2016) *Streptomyces albus* J1074/R2 (Rebets et al., 2015), *Streptomyces* sp. IB2014/011-12 (alpiniamides) (Paulus et al., 2018), *Amycolatopsis orientalis* (vancomycin) (Zmijewski & Briggs, 1989), *Actinoplanes teichomyceticus* ATCC 31121 (teicoplanin) (Horbal et al., 2012), *Streptomyces albus* subsp. *chlorinus* NRRL B-24108 (nybomycin) (Rodriguez Estevez et al., 2018), *Streptomyces rimosus* ATCC 10970 (oxytetracycline) (Pethick et al., 2013), *Streptomyces* sp. IB2014/016-6 (perquinolines) (Rebets et al., 2019), *Streptomyces lividans* ΔYA9 (usabamycins) (Ahmed et al., 2020)[Color figure can be viewed at wileyonlinelibrary.com]

TABLE 1 Strains and natural products investigated in this study and corresponding culture conditions

Strain	Natural product	Medium	Reference
Streptomyces albus J1074/R2	Pamamycins	SGG	Rebets et al. (2015)
Streptomyces lividans TK24 DG2-Km-P41hyg+	Bottromycins Undecylprodigiosin	SG	Horbal et al. (2018)
Streptomyces rimosus ATCC 10970	Oxytetracycline	GOTC	ATCC
Streptomyces albus pCinCatInt	Cinnamycins	TSB	Lopatniuk et al. (2017)
Streptomyces albus subsp. *chlorinus* NRRL B-24108	Nybomycin Usabamycins	DNPM	Myronovskyi et al. (2020)
Streptomyces sp. IB2014/011-12	Alpiniamides	TSB	Paulus et al. (2018)
Streptomyces sp. IB2014/016-6	Perquinolines	TSB	Rebets et al. (2019)
Amycolatopsis japonicum DSM 44213	Vancomycin	TSB	DSMZ
Actinoplanes teichomyceticus ATCC 31121	Teicoplanin	TSB	ATCC
Kitasatospora sp. DSM 102431	Simocyclinones	TSB	DSMZ

Abbreviations: ATCC, American Type Culture Collection; DSMZ, Deutsche Stammsammlung für Mikroorganismen und Zellkulturen (German Collection of Microorganisms and Cell Cultures).

liquid pre-cultures and main cultures, different growth media were used to meet the specific physiological demand of the investigated cells, as summarized in Table 1. Liquid TSB medium (Sigma Aldrich, pH 7.2) contained per liter: 17 g casein peptone (pancreatic), 2.5 g dipotassium hydrogen phosphate, 2.5 g glucose, 5 g NaCl, and 3 g soya peptone (papain digest.). Liquid SG medium (pH 7.2) contained per liter: 20 g glucose, 10 g soytone (Becton & Dickinson), 5 g yeast extract (Becton & Dickinson), and 2 g $CaCO_3$. Liquid SGG medium (pH 7.2) contained per liter: 10 g soluble starch (Sigma-Aldrich), 10 g glycerol, 2.5 g corn steep powder (Sigma-Aldrich), 5 g bacto peptone (Becton & Dickinson), 2 g yeast extract (Becton & Dickinson), 1 g NaCl, and 21 g MOPS. Liquid DNPM medium (pH 6.8) contained per liter: 40 g dextrin, 7.5 g soytone (Becton & Dickinson), 5 g yeast extract (Becton & Dickinson), and 21 g MOPS. Liquid GOTC medium (pH 7.0) contained per liter: 28 g corn starch (Sigma-Aldrich), 42 g soybean flour (Sigma-Aldrich), 6 g $(NH_4)_3PO_4$, 2 g $MgCl_2$, 1.5 g NaCl, 7.3 g $CaCO_3$, 10 ml 1% $ZnSO_4$, and 3.75 ml 1% $MnSO_4$. Talc (hydrous magnesium silicate, $3MgO \cdot 4SiO_2 \cdot H_2O$, 10 µm, Sigma-Aldrich) was resuspended in 50 mM Na-acetate buffer (pH 6.5), autoclaved at 121°C for 20 min, and added to the sterile medium before inoculation of selected microparticle experiments as given below (Kuhl et al., 2020).

2.3 | Cultivation

One loop of spores was scratched from a 5-day-old plate culture (incubated at 30°C) and used to inoculate a liquid pre-culture, which was grown overnight in a 500 ml baffled shake flask, filled with 50 ml medium and 30 g soda-lime glass beads (5 mm, Sigma-Aldrich). When the pre-culture had reached the late exponential phase, cells were collected (8500×g, room temperature, 5 min), resuspended in 10 ml fresh medium, and used to inoculate the main cultures, either containing talc or not. Main cultures were grown in shake flasks and in

deep-well flower plates, respectively. Shake flask cultures were incubated in 500 ml baffled shake flasks (50 ml medium) on a rotary shaker (28°C, 230 rpm, 75% relative humidity, 5 cm shaking diameter, Multitron, Infors AG). For miniaturized screening, cells were grown in 48-well flower plates (1 ml medium) using a benchtop incubator (28°C, 1300 rpm, 75% relative humidity, BioLector m2p labs). All experiments were conducted as biological triplicate.

2.4 | Quantification of cell concentration

The cell dry weight (CDW) of *S. lividans* was measured as follows. Cells were collected (10,000×g, 4°C, 10 min), washed twice with 15 ml deionized water, and freeze-dried (Kuhl et al., 2020). Subsequently, the dry biomass was gravimetrically determined (Gläser et al., 2020). In microparticle cultivations of *S. lividans*, biomass data were corrected for the amount of talc added (Kuhl et al., 2020)

2.5 | Quantification of glucose

Glucose was quantified by HPLC (1260 Infinity Series, Agilent), using an Aminex HPX-87H column (300 × 7.8 mm; Bio-Rad) as stationary phase and 7 mM H_2SO_4 as mobile phase (55°C, 0.7 ml min⁻¹). Refraction index measurement was used for detection, and external standards were used for quantification (Kuhl et al., 2020).

2.6 | Microscopy

The 5 µl culture broth was transferred onto a glass for bright-field microscopy (Olympus IX70 microscope). The software ImageJ 1.52 (Schneider et al., 2012) was used to automatically determine the size

of pellets formed during growth (Kuhl et al., 2020). At least 150 aggregates were analyzed per sample.

2.7 | Natural compound extraction and quantification

The different natural products investigated in this study (Table 1) were extracted from culture broth using a two-step process (Kuhl et al., 2020). In short, 500 µl broth was mixed with 500 µl acetone and incubated for 15 min (1000 rpm, room temperature, Thermomixer F1.5, Eppendorf). Subsequently, ethyl acetate (500 µl) was added to extract bottromycin, undecylprodigiosin, pamamycins, vancomycin, teicoplanin, alpiniamides, perquinolines, simocyclinones usabamycins, and nybomycin, respectively, whereas 1-butanol (500 µl) was added to extract cinnamycins and thioholgamide A. Each mixture was incubated for 15 min under the same conditions. Afterward, the organic phase was collected ($20,000\times g$, room temperature, 5 min), and the solvent was evaporated under a laminar nitrogen stream. Extracts were re-dissolved in methanol and clarified from debris ($20,000\times g$, 4°C, 10 min). Subsequently, the analytes of interest were quantified, using HPLC-ESI-MS (C18 column, Vision HT C18 HighLoad, 100×2 mm, 1.5 µm, Dr. Maisch, Ammerbuch-Entringen, Agilent Infinity 1290, AB Sciex QTrap 6500). The individual chromatographic and mass spectrometric settings for each investigated compound are summarized in Table S1. To extract oxytetracycline, 250 µl culture broth was adjusted to pH 1.5 with 37% HCl and centrifuged twice ($21,000\times g$, 15 min, 4°C). The resulting supernatant was analyzed by HPLC (Agilent 1260 Infinity Series, Agilent Technologies) on a C18 column (Nucleodur C18 Isis, 100×3 mm, 3 µm, Macherey-Nagel). Oxytetracycline was detected by a diode array detector (275 nm), and external standards were used for quantification.

2.8 | Extraction and quantification of intracellular amino acids

Intracellular amino acid sampling was done using fast vacuum filtration with nitrocellulose filters (0.2 µm pore size, Sartorius) (Wittmann et al., 2002). After vacuum filtration of 1 ml culture broth through a nitrocellulose filter (0.2 µm pore size, Sartorius), the cell-containing filter was washed twice with 15 ml 1.5% NaCl, transferred into a plastic cup containing 2 ml 200 µM α-aminobutyrate as internal standard for later quantification, and incubated 15 min at 100°C for amino acid extraction. Subsequently, the obtained extract was cooled on ice, and clarified from debris ($20,000\times g$, 4°C, 5 min). The amino acids were quantified by HPLC using α-aminobutyrate as internal standard and pre-column derivatization with o-phthaldialdehyde (Schwechheimer et al., 2018).

2.9 | Transcriptome analysis

Total RNA was isolated using the Quick-RNA Miniprep Plus kit (Zymo Research). After DNase treatment, the obtained RNA was purified (RNA Clean & Concentrator-5 kit, Zymo Research) and quantified (DropSense 16, Trinean NV). The quality of the RNA was validated (RIN > 9) (RNA 6000 Nano kit, Agilent 2100 Bioanalyzer, Agilent Technologies). To construct whole transcriptome complementary DNA (cDNA) libraries, 2.5 µg of total RNA each was depleted of ribosomal RNA (rRNA) (Ribo-Zero rRNA Removal Kit (Bacteria), Illumina). Successful rRNA removal was validated (Agilent RNA Pico 6000 kit, Agilent 2100 Bioanalyzer, Agilent Technologies). The obtained messenger RNA (mRNA) was converted into a cDNA library according to the TruSeq Stranded mRNA Sample Preparation guide (Illumina). Appropriate cDNA quality and quantity was validated (Agilent High Sensitivity DNA kit, Agilent 2100 Bioanalyzer, Agilent Technologies). Sequencing was performed on an Illumina HiSeq. 1500 instrument using 70 bases read length (Illumina).

The obtained reads were mapped to the *S. lividans* D/G2 genome sequence (CP071123), which is based on the re-annotated *S. lividans* TK24 genome (Droste et al., 2021), using BOWTIE2 under standard settings (Langmead & Salzberg, 2012), except for increasing the maximally allowed distance for paired reads to 600 bases. To visualize read alignments, the software READXPLORER 2.2.3 (Hilker et al., 2016) was used. To count reads mapping to gene features, FEATURECOUNTS v.2.0.0 (Liao et al., 2014) was applied using the parameters -M -O, and -s 1. Quality control of the processed data sets was performed using DESEQ. 2 (Love et al., 2014), including calculation of sample-to-sample distances and principal component analysis. In addition, DESEQ. 2 was used to calculate DGE data sets. Raw data sets (sequenced reads) as well as processed data sets (input matrix and normalized read counts from DESEQ. 2) are available from GEO (GSE168044). For statistical analysis, Student's t-test was carried out and the data were filtered for genes with a $\log_2$-fold change ≥ 1 ($p \leq 0.05$) (Kuhl et al., 2020). RNA extraction and sequencing were conducted as biological triplicates for each strain.

3 | RESULTS

3.1 | Microparticles enhance the production of bottromycin A2, methyl-bottromycin A2, and undecylprodigiosin in recombinant *S. lividans*

To investigate the effect of the microparticles in detail, a bottromycin-producing mutant of *S. lividans* was studied in liquid culture with 10 g L^{-1} talc (Figure 2), an amount recently found optimal for the related strain *S. albus* J1074/R2 (Kuhl et al., 2020). A culture without talc served as control. The recombinant strain *S. lividans* TK24 DG2-Km-P41hyg+ expressed a refactored version of the *bot* cluster from *S. sp.* BC16019 (Huo et al., 2012) under control of two back-to-back synthetic promoters (Horbal et al., 2018). In the control culture, the strain grew from early on and reached a maximum biomass concentration of 7.4 (g CDW) L^{-1} after 48 h (Figure 2a). Then, growth stopped. However, the cells continued to consume glucose which was depleted after 120 h. The mature bottromycins, that is, bottromycin A2 and methyl-bottromycin A2,
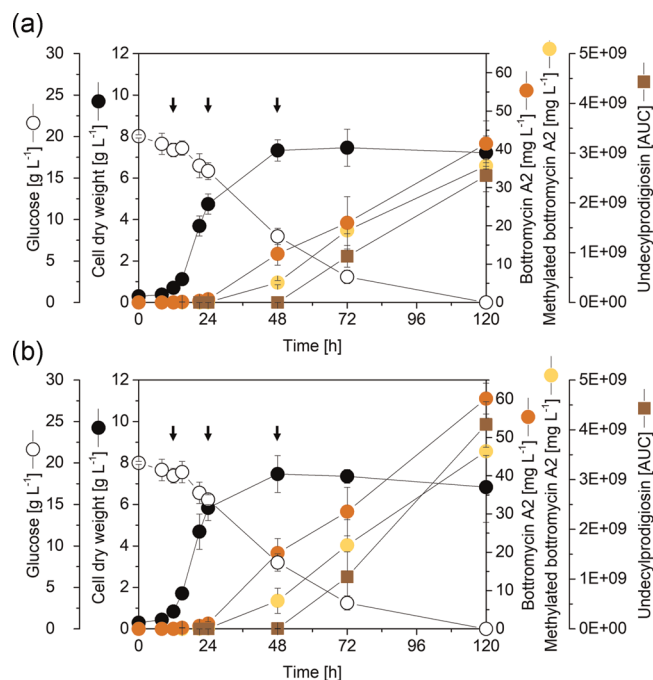
FIGURE 2 Impact of talc microparticles on growth and natural product formation in *Streptomyces lividans* TK24 DG2-Km-P41hyg+. The data show growth and production dynamics of a control culture without microparticles (a) and a microparticle-supplemented culture (10 g L^{-1} talc) (b). The arrows indicate the sampling time points for metabolome analysis (pre-bottromycins, bottromycin shunt products, intracellular amino acids), transcriptome analysis (RNA sequencing), and/or morphology analyzes. n = 3 [Color figure can be viewed at wileyonlinelibrary.com]

started to accumulate after approximately 20 h. The two products reached final titers of 42 mg L^{-1} and 35 mg L^{-1}, respectively. In contrast, bottromycin B and D were not observed. Alongside bottromycin, *S. lividans* formed undecylprodigiosin, a native alkaloid (van Wezel et al., 2000). The production of the latter started after 48 h and continued until the end of the process.

In comparison, the microparticle supplemented culture achieved significantly increased product titers. The final level of bottromycin A2 (60 mg L^{-1}) was 43% higher than that in the control, while the methyl-bottromycin A2 titer (46 mg L^{-1}) was increased by 31%. Increased product levels already occurred after 48 h. In addition, undecylprodigiosin production was increased by the particle supplementation (particularly during later stages of the cultivation) and resulted in a 64% increased final titer. The enhanced accumulation of the red pigment was even visible by the eye (Figure 3). Talc-supplemented cells appeared red, while cells from the control culture were less-intensively colored.

Interestingly, biomass formation and glucose consumption remained rather unchanged between the talc-supplemented culture and the control. However, talc had a major impact on cellular morphology. Grown without talc, the recombinant producer formed larger pellets with an average diameter of 390 ± 118 µm (Figure 3), while cellular aggregates in the talc supplied culture were

significantly smaller and exhibited a 40% reduced pellet diameter of 279 ± 49 µm. In later stages of the cultivation, the morphology differed also in inner structure (Figure S1). The cell aggregates in the control reached up to 1 mm in diameter and pellets appeared decomposed inside. Pellets of the talc culture were less than half in size and exhibited an intact and denser structure. Further tests revealed a production optimum for total bottromycins (109 ± 24 mg L^{-1}) at 15 g L^{-1} talc (Figure S2). Higher talc levels were found detrimental.

3.2 | Microparticles do not affect bottromycin precursor availability during initial ribosomal translation but significantly change the abundance of intermediates of the posttranslational modification pathway

We hypothesized that the increased bottromycin titers could result from a higher precursor availability, as recently shown for other natural products (Gläser et al., 2020; Kuhl et al., 2020; Ser et al., 2016; Tang et al., 1994; Thykaer et al., 2010). Therefore, we analyzed the level of intracellular amino acids during growth (12 h, Figure 4b) and production (48 h, Figure 4c), including the building blocks of mature bottromycin A2: glycine, L-proline, L-valine, L-phenylalanine, L-aspartate, and L-cysteine (highlighted in blue in Figure 4b,c). Talc microparticles had virtually no effect: all intracellular amino acid pools remained unchanged. Generally, L-glutamate was most abundant, followed by L-alanine. Taken together, talc-enhanced bottromycin production was obviously not triggered by increased amino acid availability at the level of the initial ribosomal formation of the peptide backbone.

However, the talc particles affected the accumulation of biosynthetic intermediates from the posttranslational part of the biosynthetic pathway, including pre-forms of bottromycin and so-called shunt (degradation) products which appeared in addition to the mature bottromycins (carrying all major posttranslational modifications) (Figure 4a). Talc significantly increased the abundance of the pre-forms, that is, nonmethylated pre-bottromycin (*m/z* 855.4) and methylated pre-bottromycin (*m/z* 869.4). In contrast, the level of incomplete precursor peptides (*m/z* 452.2) was substantially reduced by talc addition, and non-cyclized shunt products exhibited a similar trend, although less significant.

3.3 | Microparticles rebalance the expression of individual bottromycin cluster genes

It was now interesting to see how bottromycin synthesis was affected on the transcriptional level. For this purpose, global transcription profiling of bottromycin-producing *S. lividans* was performed using RNA sequencing (Figure S3). The transcriptome of a talc supplied culture (10 g L^{-1}) was compared to that of a control at different stages of the cultivation: exponential growth (12 h), early production (24 h), and main production (48 h). Sample-level quality
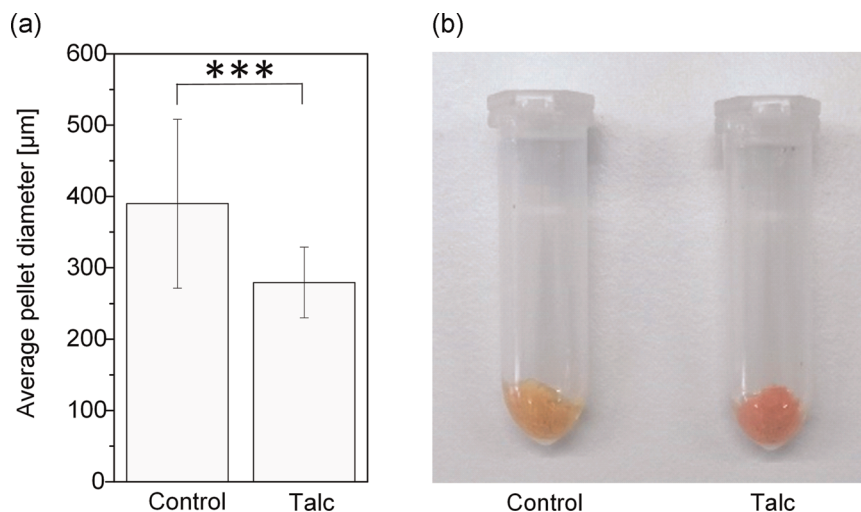
FIGURE 3 Impact of talc microparticles on the cellular morphology of *Streptomyces lividans* TK24 DG2-Km-P41hyg + in liquid culture. The data show the average pellet diameter of a microparticle-supplemented culture ($10\,g\,L^{-1}$ talc) and a control culture without microparticles at production start (24 h) (a, ***$p < 0.001$, $n = 150$). In addition, the pellet color of control culture and talc supplied culture after 5 days of incubation is shown, reflecting enhanced production of the red pigment undecylprodigiosin in the presence of talc (b) [Color figure can be viewed at wileyonlinelibrary.com]

control revealed excellent reproducibility (Figures 5 and S4). The individual replicates of all samples closely clustered together so that the observed expression differences could be fully attributed to the different experimental conditions. During early production, the expression of all bottromycin cluster genes remained unchanged in the control, whereas *botP*, was upregulated in the talc culture (2.0-fold) (Figure 6). During the main production phase, most bottromycin cluster genes were changed in expression. Obviously, the microparticles re-balanced the expression of the cluster in the microbe: *botAH* was specifically increased in the talc culture (2.4-fold) and *botC* and *botA* remained constant, while the latter two genes were found upregulated in the control (2.1-fold and 2.3-fold, respectively). Other genes equally behaved under both conditions: *botRMT1* was downregulated (0.4-fold), whereas *botCD, botH, botT, botRMT2*, and *botRMT3* remained unaffected over the entire process. It was interesting to note that the expression of the cluster was only weakly driven by the synthetic promoters (Figure S5a), but largely relied on the promoter of the hygromycin marker gene *hygR* (P_{hygR}), inserted in between them (Figure S5b). In addition, a so far unknown but apparently even stronger promoter downstream of *hygR*, designated P_{AS}, transcribed the cluster in the opposite (antisense) direction (Figure S5c).

3.4 | Microparticles accelerate morphological development and aging of *S. lividans*

On a global level, talc-supplied and non-supplied cells massively changed their gene expression during the process (Figure S3). In the control culture, 5% of all 7751 genes (414) were modulated in expression during the shift from growth to early production. The number of altered genes was increased to 2790 (36%) during the main production phase indicating a major shift of the cellular program at this stage. The expression changes, observed after 48 h, included prominent regulators of morphology and secondary metabolism, such as *ssgAB, chpABCDEFGH, rdlAB, rarABCDE, eshA*, and corresponding sigma factors (Tables 2 and 3), indicating ongoing morphological development and aging of the liquid-culture, a typical behavior of Streptomycetes, also observed in other species (van Dissel et al., 2014).

For the talc-amended culture, the transcription profile changed faster, and the dynamics involved more genes (Figure S3). The observed changes were related to the cultivation stage (Figure 5). Notably, the microparticles accelerated the shift in expression, leading to specific differences already during early production which indicated an accelerated morphological development. The number of genes, altered in expression after 24 h in the microparticle culture (1094 genes, 14%), was almost three times higher than that in the control. Key morphology genes and regulators, including *ssgA* (*SLIV_18635*, 3.3-fold), *ssgB* (*SLIV_30050*, 2.0-fold), *wblA* (*SLIV_20395*, 2.8-fold), *sigN* (*SLIV_18240*, 2.5-fold), and *bldN* (*SLIV_21180*, 3.2-fold, among others, were exclusively activated after 24 h in the presence of talc (Tables 2 and 3). In addition, various native biosynthetic genes for secondary metabolites were upregulated by talc at this early stage (Figure S6). During the main production after 48 h, the expression level of genes associated to morphology and secondary metabolism appeared rather similar with and without talc, although slight differences remained and totally more genes (38%, 2979) were modulated in the talc process. Interestingly, not even one single gene showed a significantly altered expression with talc supply during the growth phase (Figure S4).
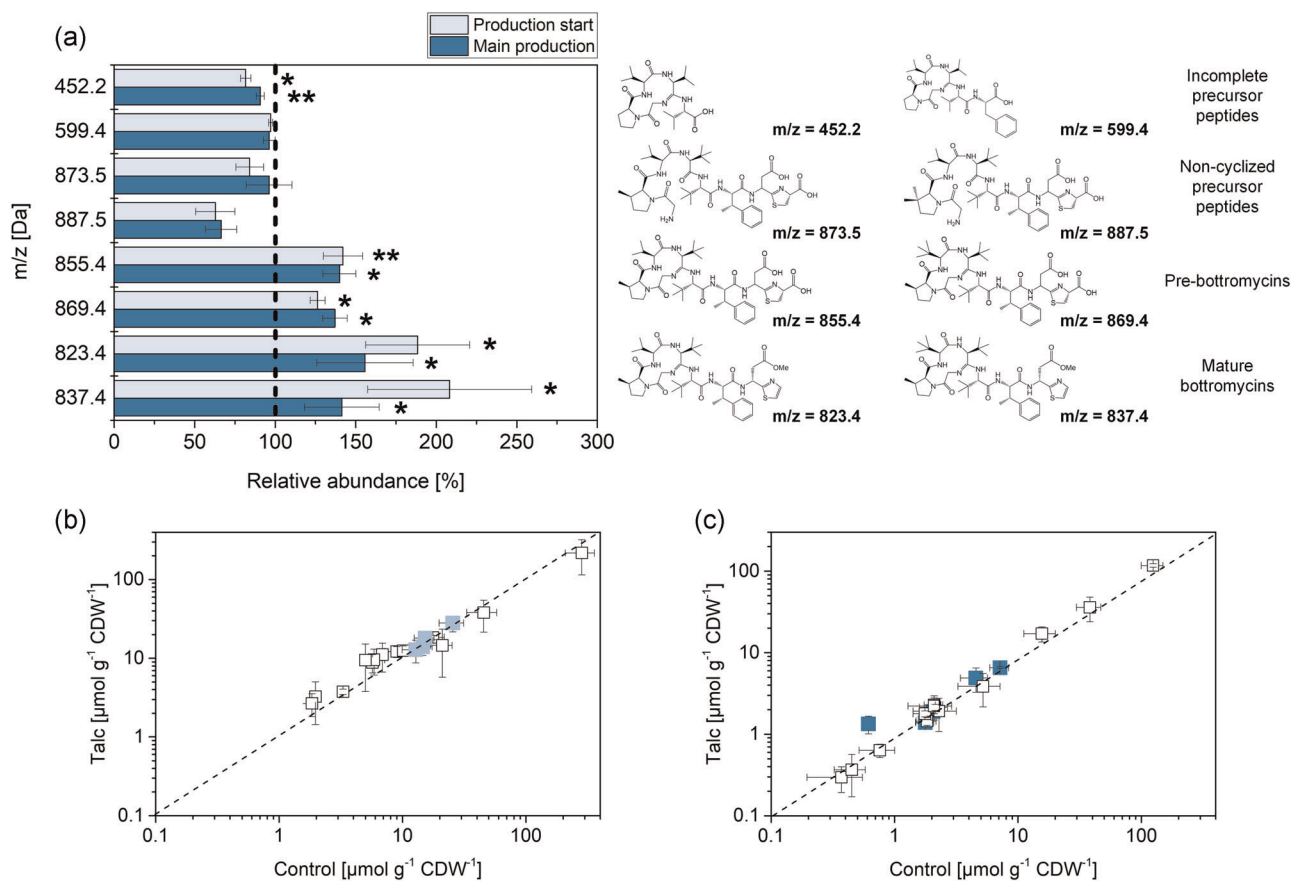
FIGURE 4 Metabolomic impact of talc microparticles on bottromycin-producing *Streptomyces lividans* TK24 DG2-Km-P41hyg+. The data show relative changes in the level of bottromycin pathway intermediates (a) and intracellular amino acids (b), (c), upon addition of talc microparticles to the medium ($10 \, \text{g L}^{-1}$). (a) The data show pre-bottromycin (m/z = 855.4), methylated pre-bottromycin (m/z = 869.4), four shunt products (m/z = 452.2, m/z = 599.4, m/z = 873.5, and m/z = 887.5), final mature bottromycin A2 (m/z = 823.4), and methylated-bottromycin A2 (m/z = 837.4), previously described (Crone et al., 2016; Vior et al., 2020). The data reflect the production start (24 h) and the major production phase (48 h), and the control culture (without talc), set to 100%, is shown as dashed line (*$p \leq 0.05$, **$p \leq 0.01$). The intracellular amino acid pools reflect the growth phase (12 h, b) and the major production phase (48 h, c). The amino acids that are incorporated into mature bottromycins (L-glycine, L-proline, L-valine, L-phenylalanine, L-aspartate, and L-cysteine) are highlighted in blue. The intracellular amino acid pools during early production were not found significantly changed (data not shown) [Color figure can be viewed at wileyonlinelibrary.com]
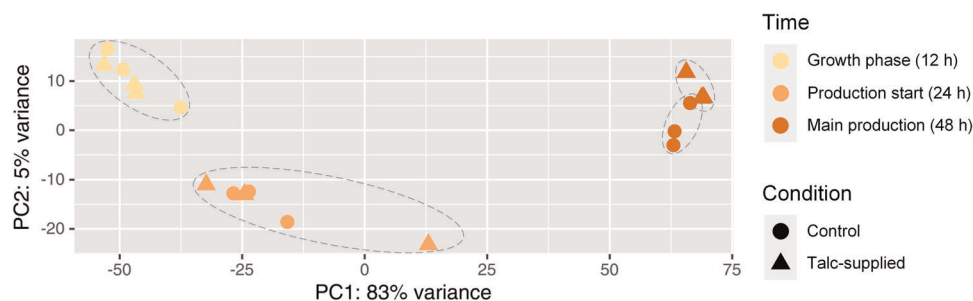
FIGURE 5 Statistical evaluation of gene expression profiles of *Streptomyces lividans* TK24 DG2-Km-P41hyg + using PCA. Global transcription profiling of the cultures was conducted using RNA sequencing during growth (12 h) and bottromycin production (24 h, 48 h) in the presence of talc ($10 \, \text{g L}^{-1}$) and without talc (control). For calculation of normalized read counts, the raw read count data were processed by DESeq. 2 (Love et al., 2014), including regularized log transformation (with blind dispersion estimation enabled). Subsequently, PCA was performed and visualized using ggplot2 (Wickham et al., 2016). $n = 3$ [Color figure can be viewed at wileyonlinelibrary.com]
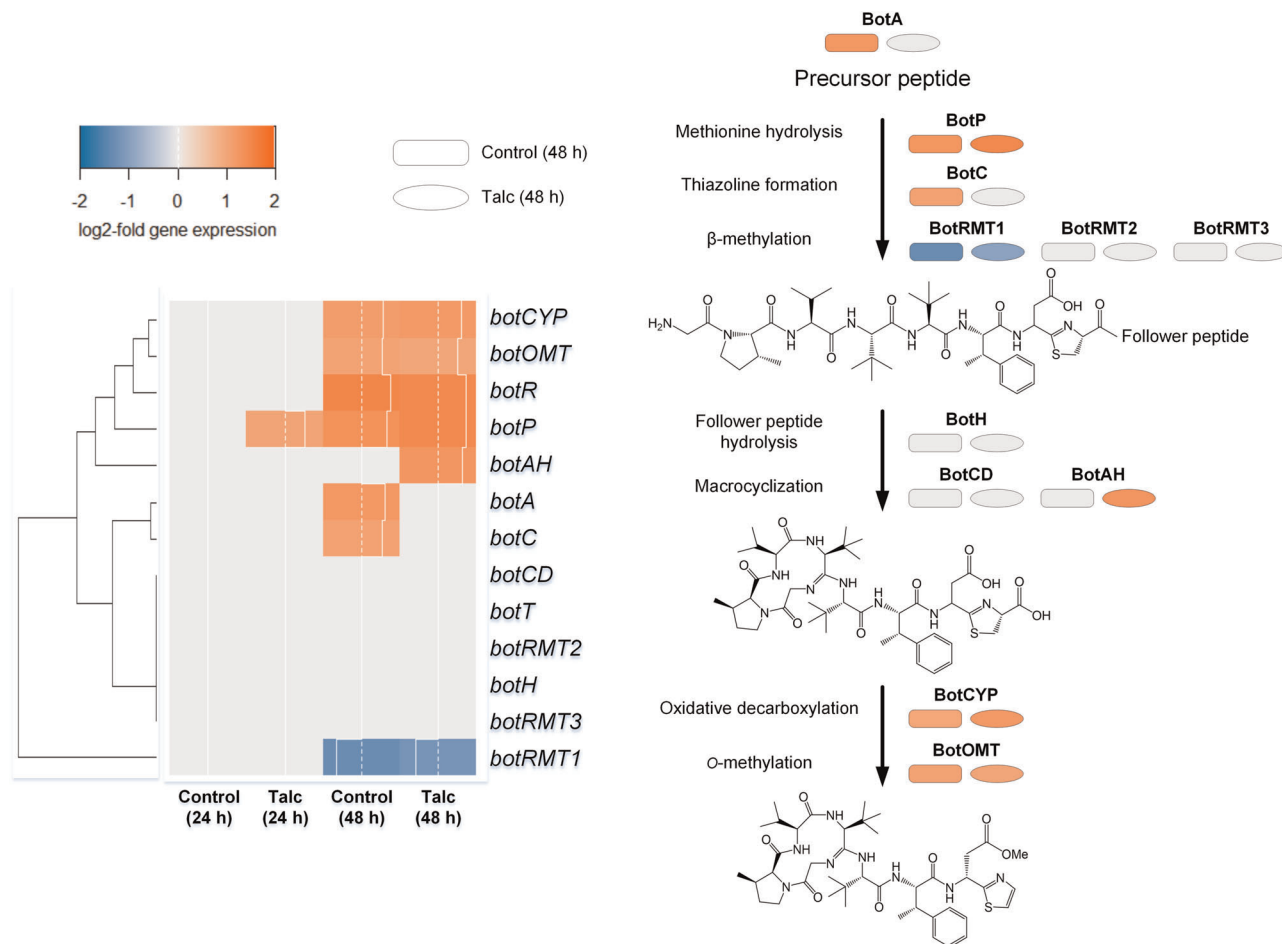
FIGURE 6 Hierarchical cluster analysis of expression dynamics of bottromycin biosynthetic pathway genes in *Streptomyces lividans* TK24 DG2-Km-P41hyg+. Samples were taken from a control and a talc supplied culture (10 g L^{-1}) during growth (12 h), production start (24 h), and major production phase (48 h). The expression level of the control during growth (12 h) was set as reference. The bottromycin cluster comprised the genes *botA*, encoding the precursor peptide; *botP*, leucyl-aminopeptidase; *botC*, YcaO domain protein; *botRMT1*, radical SAM; *botRMT2*, radical SAM; *botRMT3*, radical SAM; *botCD*, YcaO domain protein; *botAH*, aminohydrolase; *botH*, hydrolase; *botCYP*, CYP450 enzyme; *botOMT*, *O*-methyl transferase; *botT*, multidrug transporter; *botR*, transcriptional regulator (Huo et al., 2012). *n* = 3 [Color figure can be viewed at wileyonlinelibrary.com]

3.5 | The addition of talc to various *Streptomyces* cultures enhances the formation of natural products up to thirteen-fold

Given the stimulating effects of microparticles on bottromycin production in *S. lividans* (this study) and pamamycin production in *S. albus* (Kuhl et al., 2020), we now tested the concept on a broader scale. To facilitate the screening, we miniaturized production and established cultures at the microliter scale in a parallelized microtiter plate incubator. For appropriate mixing and oxygen transfer, the microtiter plates contained flower-shaped wells, optimized in geometry for the applied 3 mm shaking diameter of the instrument (Funke et al., 2009). To validate the microliter scale against conventional shake flasks, a first round of experiments was conducted for *S. lividans* TK24 DG2-Km-P41hyg + (Figure 2) and *S. albus* J1074/R2 (Kuhl et al., 2020), for which the stimulating microparticle effects had been already proven in shake flasks. Both strains were

grown in microtiter plates over 5 days at different levels of talc (0–50 g L^{-1}) on their preferred medium (Table 1), followed by culture harvesting, natural product extraction and HPLC-ESI-MS analysis. As shown, the production of the bottromycins and undecylprodigiosin by *S. lividans* TK24 DG2-Km-P41hyg + , as well as the production of pamamycins by *S. albus* J1074/R2 was significantly enhanced by talc (Figure 7). Obviously, the miniaturized scale yielded the same picture as observed before for the 50 mL scale in shake flasks, although titers were somewhat lower, and it seemed appropriate to screen for the microparticle-based effects.

Subsequently, we investigated the production of different classes of natural products in a variety of *Streptomyces* species at the miniaturized scale including cinnamycins, another family of RiPPs (in addition to bottromycin), alpiniamides, another family of polyketides (in addition to pamamycins), the tetracycline derivative oxytetracycline, usabamycins of the anthramycin-type, the tetrahydroisochinoline-type perquinolines, and nybomycin, exhibiting a so far unique structure

TABLE 2 Gene expression profiling of recombinant *Streptomyces lividans* TK24 DG2-Km-P41hyg + during growth (12 h) and bottromycin production (24 h and 48 h) in the presence of talc (10 g L^{-1}) and without talc (control)

Gene	Annotation	Common gene name	Control (24 h)	Talc (24 h)	Control (48 h)	Talc (48 h)
SLIV_00805	Nucleotide-binding protein	*eshA*	0.0	0.0	4.9	4.8
SLIV_03010	Hypothetical protein	*chpB*	0.0	0.0	4.6	5.6
SLIV_04280	Regulatory protein	*absR2*	0.0	0.0	3.0	4.4
SLIV_04285	Regulatory protein	*absR1*	0.0	0.0	2.2	2.0
SLIV_09200	Response regulator	*redZ*	0.0	0.0	1.5	1.5
SLIV_09220	Transcriptional regulator RedD	*redD*	0.0	0.0	2.7	2.9
SLIV_09960	BldB	*bldB*	0.0	1.2	1.2	1.1
SLIV_12810	ABC transporter integral membrane protein BldKC	*bldKC*	0.0	−1.6	−1.6	−1.7
SLIV_12810	ABC transporter lipoprotein BldKB	*bldKB*	0.0	0.0	−1.3	−1.5
SLIV_12810	ABC transporter integral membrane protein BldKA	*bldKA*	0.0	0.0	−1.2	−1.5
SLIV_12835	Hypothetical protein	*act*II-ORF4	0.0	0.0	4.6	3.7
SLIV_14520	Two component regulator	*bldM*	0.0	1.6	4.9	5.1
SLIV_16305	Regulatory protein	*afsR*	0.0	1.1	1.1	1.5
SLIV_16310	Hypothetical protein	*afsS*	0.0	0.0	0.0	0.0
SLIV_17970	Hypothetical protein	*bldC*	0.0	0.0	1.5	1.5
SLIV_18635	SsgA	*ssgA*	0.0	1.7	4.2	4.1
SLIV_20395	WhiB-family transcriptional regulator	*wblA*	0.0	1.5	4.4	4.5
SLIV_21560	Two component system response regulator	*absA2*	0.0	0.0	−1.8	−2.0
SLIV_21565	Two component sensor kinase	*absA1*	0.0	0.0	0.0	0.0
SLIV_21605	Transcriptional regulator	*cdaR*	0.0	2.4	3.6	3.4
SLIV_23715	AraC family transcription regulator	*bldH*	0.0	0.0	1.6	1.8
SLIV_24075	Secreted protein	*rdlB*	0.0	0.0	5.1	5.2
SLIV_24080	Hypothetical protein	*rdlA*	0.0	3.9	10.0	10.6
SLIV_24085	Hypothetical protein	*chpD*	0.0	3.1	8.2	8.9
SLIV_24090	Hypothetical protein	*chpA*	0.0	0.0	6.0	7.1
SLIV_24145	Putative secreted protein	*chpF*	0.0	0.0	5.3	6.2
SLIV_24175	Hypothetical protein	*chpG*	0.0	0.0	7.5	7.4
SLIV_28720	Putative secreted protein	*chpE*	0.0	0.0	5.2	5.0
SLIV_29370	Putative secreted protein	*chpH*	0.0	0.0	4.2	3.3
SLIV_29375	Secreted protein	*chpC*	0.0	0.0	4.9	4.4
SLIV_29590	Hypothetical protein	*rarA*	0.0	0.0	4.9	5.0
SLIV_29595	Hypothetical protein	*rarB*	0.0	0.0	6.4	6.5
SLIV_29600	Hypothetical protein	*rarC*	2.0	2.0	8.1	7.7
SLIV_29605	ATP-GTP binding protein	*rarD*	1.8	1.7	7.7	7.5
SLIV_29610	Cytochrome P450	*rarE*	0.0	1.8	7.8	7.8
SLIV_30050	Regulator	*ssgB*	0.0	1.0	1.9	1.9

Note: The table lists the expression of genes involved in the regulation of morphology and secondary metabolism. The values correspond to log$_2$-fold expression changes and refer to the control (12 h) as reference. n = 3.

TABLE 3 Transcriptional changes of selected sigma factors in *Streptomyces lividans* TK24 DG2-Km-P41hyg + during growth (12 h) and bottromycin production (24 h and 48 h) in the presence of talc ($10\,\mathrm{g\,L^{-1}}$) and without talc (control)

Gene	Annotation	Control (24 h)	Talc (24 h)	Control (48 h)	Talc (48 h)
SLIV_03325	Sigma factor	0.0	0.0	3.1	3.4
SLIV_03750	RNA polymerase sigma factor	0.0	0.0	3.9	4.4
SLIV_10445	RNA polymerase sigma factor WhiG	0.0	0.0	2.1	2.7
SLIV_12150	SigH protein	0.0	0.0	1.4	1.5
SLIV_14045	ECF sigma factor	0.0	0.0	−2.5	−2.1
SLIV_14515	RNA polymerase sigma factor SigD	0.0	0.0	2.8	2.9
SLIV_16170	RNA polymerase sigma factor	0.0	0.0	1.5	1.2
SLIV_16385	RNA polymerase sigma factor	0.0	1.2	2.4	2.9
SLIV_18240	RNA polymerase sigma factor SigN	0.0	1.3	2.0	1.9
SLIV_21180	ECF sigma factor BldN	0.0	1.7	6.4	6.4
SLIV_22925	RNA polymerase sigma factor SigU	0.0	0.0	3.9	5.0
SLIV_23960	sigma factor	0.0	0.0	2.5	2.2
SLIV_25360	RNA polymerase principal sigma factor HrdA	0.0	0.0	7.4	7.1
SLIV_29905	RNA polymerase sigma factor	0.0	6.4	6.7	7.2
SLIV_31410	RNA polymerase ECF sigma factor	0.0	0.0	2.3	0.0
SLIV_33600	ECF family RNA polymerase sigma factor	3.1	1.8	6.9	6.7
SLIV_33610	ECF family RNA polymerase sigma factor	0.0	0.0	2.8	2.5
SLIV_36925	Sigma factor LitS	0.0	0.0	1.7	2.4

Note: The values correspond to $\log_2$-fold expression changes and refer to the control (12 h) as reference. $n = 3$.

(Figure 7). Talc addition enhanced natural product formation in six out of nine cases (67%) resulting in increased titers for cinnamycins, bottromycins, undecylprodigiosin, pamamycins, oxytetracycline, and usabamycins. In each case, a production optimum could be identified. Interestingly, the optimal talc concentration strongly differed for each strain and compound. Among all products, the highest increase was observed for the alkaloid undecylprodigiosin (thirteen-fold, at $20\,\mathrm{g\,L^{-1}}$ talc). For certain products, the microparticles not only influenced the overall yield, but specifically altered the spectrum of the formed derivatives. This resulted in notable changes, including enhancing and diminishing effects on derivatives that were minor side products in the control without talc. As example, usabamycin C production was more than doubled by the addition of $10\,\mathrm{g\,L^{-1}}$ talc, whereas the deoxycinnamycin level was reduced three-fold, when $20\,\mathrm{g\,L^{-1}}$ talc was present.

3.6 | Microparticles boost natural product formation across actinobacterial genera and families

Finally, the applicability of the microparticle approach was tested for other actinobacteria, outside of the genus of *Streptomyces* (Figure 7). Therefore, we examined the production of two glycopeptides

(vancomycin and teicoplanin) and one angucyclinone-type antibiotic (simocyclinone), which were formed by *Amycolatopsis japonicum* DSM 44213 (vancomycin), *Actinoplanes teichomyceticus* ATCC 31121 (teicoplanin), and *Kitasatospora sp.* (simocyclinone). Talc addition boosted formation of all products in all three strains. Interestingly, the positive effects were found for native as well as for heterologous producers. For teicoplanin, the addition of talc was even crucial since the compound was barely detectable in the control. As a result of talc addition, the enhancement was almost 100-fold. As observed for the *Streptomyces* strains, the optimum amount of talc was different for the different strains.

4 | DISCUSSION

4.1 | Microparticle-enhanced production provides bottromycins at a next level of performance and adds remarkable potential to drug development and further biosynthetic studies

As shown, talc microparticles significantly increased the production of the macrocyclic peptides bottromycin A2 and Met-bottromycin A2
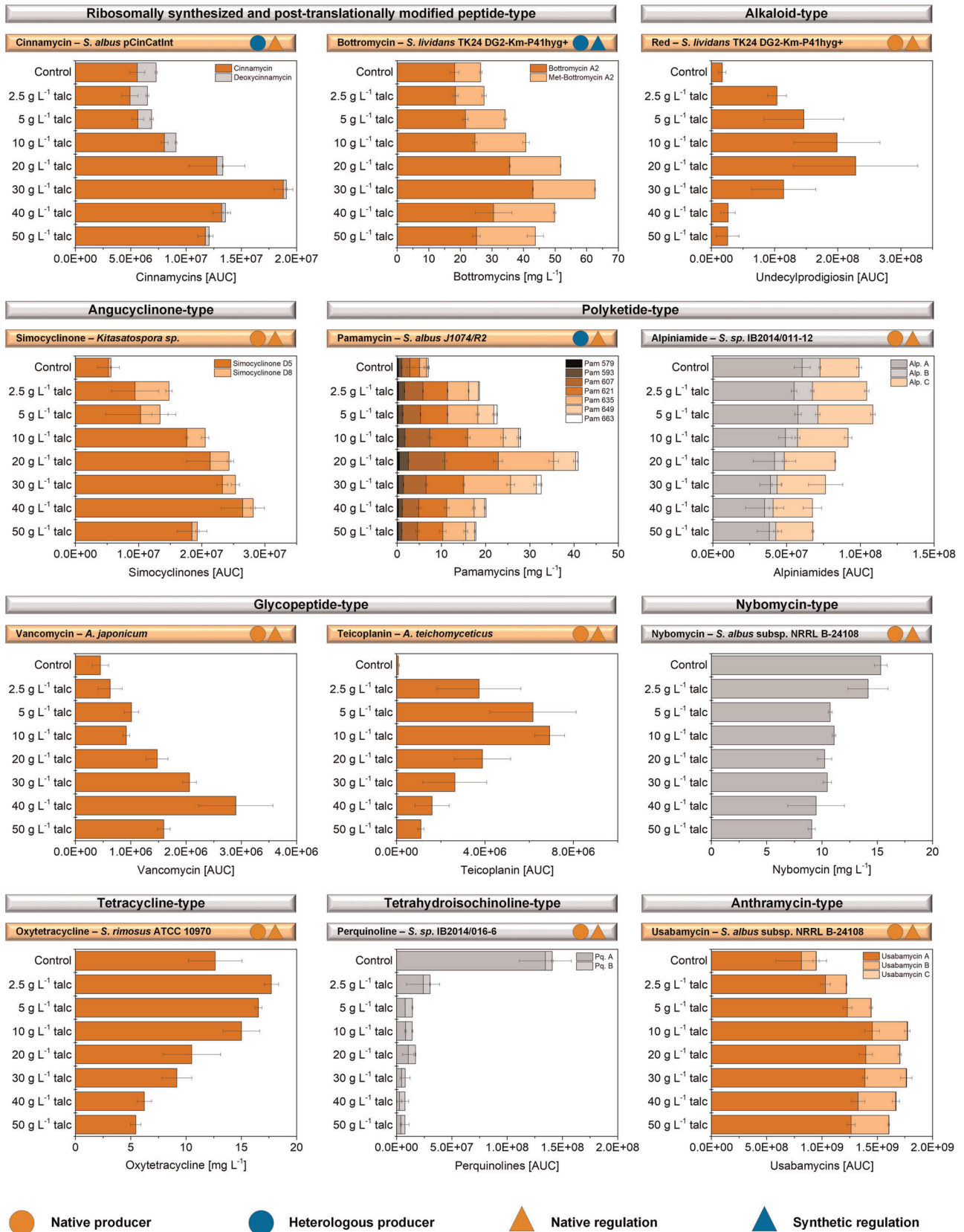
FIGURE 7 (See caption on next page)

in recombinant *S. lividans* TK24 DG2-Km-P41hyg + (Figure 2). Generally, bottromycins are difficult to obtain and their research has developed into a "nightmare" over the past 65 years (Kazmaier, 2020). Various homologous as well as heterologous producers provide bottromycins only in the low milligram range and even below 1 mg L^{-1} (Crone et al., 2016; Horbal et al., 2018; Huo et al., 2012). Due to this, improvement of titer and yield is regarded crucial (Vior et al., 2020), especially as the pathway seems inefficient in laboratory conditions (Crone et al., 2016; Eyles et al., 2018). In this study, the refactored synthetic strain *S. lividans* TK24 DG2-Km-P41hyg +, apparently among the top bottromycin producers available (Franz et al., 2021), reached 109 mg L^{-1} bottromycins of the A2 type in the presence of 15 g L^{-1} talc, exceeding all previously reported efforts. This achievement will greatly support drug development and further biosynthetic studies of bottromycins and derivatives therefrom (Vior et al., 2020). It also demonstrates that the particle approach can be successfully used to boost the performance of even top-level microbial cell factories.

4.2 | Microparticle-enhanced production of bottromycins in recombinant *S. lividans* is supported by re-balanced expression of individual bottromycin cluster genes driven by a complex promoter architecture

The obtained genomic, transcriptomic, and metabolomic data sets were now integrated to understand the involved molecular processes on a systems level (Kohlstedt et al., 2014). Resequencing of the bottromycin cluster verified the previously designed architecture with a synthetic bidirectional promotor cassette in between the left and the right part of the bottromycin cluster (Horbal et al., 2018). While precursor availability on the amino acid level could be ruled out as a limiting factor (Figure 4b,c), the talc-induced increase of pre-bottromycins together with the simultaneous decrease of non-cyclized shunt products from the upper pathway, indicated a higher efficiency of the posttranslational modification process (Figure 4a). Notably, this was accompanied by a few significant changes in gene expression. Previous studies showed that the main limiting factor in

bottromycin production, at least in the native host *S. scabies*, is the posttranslational maturation of the precursor peptide (Vior et al., 2020) and that the pathway inefficiently stalls at numerous biosynthetic steps (Crone et al., 2016). We conclude that the increased production efficiency in talc-supplied cultures largely resulted from the specifically increased expression of the aminohydrolase of the cluster (encoded by *botAH*, 2.4-fold, 48 h, Figure 6), responsible for the unique amidine-forming macrocyclodehydration of the molecule (Huo et al., 2012). Since this step follows after β-methylation of the valine, proline, and phenylalanine residues in the forming peptide, catalyzed by BotRMT1, BotRMT2, and BotRMT3 (Figure 6), this link nicely explains that the titer of both bottromycin derivatives was increased simultaneously (Crone et al., 2016; Horbal et al., 2018).

It appears likely that also the lower abundance of *botA*, encoding for precursor peptide (Figure 6) helped to balance biosynthesis, as previous attempts to increase precursor peptide levels were not found suitable to trigger bottromycin A2 synthesis, (Horbal et al., 2018; Vior et al., 2020). Taken together, fine-tuned re-balancing of the expression of individual cluster genes obviously mediated the improved biosynthesis. This picture differs largely from that obtained for talc-enhanced pamamycin production in *S. albus*, where the entire gene cluster was activated, up to 1000-fold (Kuhl et al., 2020). Likely, the difference originated from the different expression control strategies: the expression control of the bottromycin cluster in *S. lividans* was of synthetic nature (Horbal et al., 2018), whereas the pamamycin cluster was expressed under its native control (Kuhl et al., 2020). Hereby, it appeared surprising that the bottromycin cluster was affected at all, as the synthetic design was expected to uncouple expression from the host metabolism. A close inspection of the RNA sequencing data revealed that the expression control was much more complex than expected (Figure S5). It was only weakly driven by the synthetic promoters but largely relied on the highly active promoter of the hygromycin marker gene *hygR*, inserted in between of them, and transcribing the right cluster genes (Figure S5b). In addition, a so far unknown but apparently even stronger antisense promoter sequence (P$_{AS}$) downstream of *hygR*, transcribed the cluster in the opposite direction and expressed the left cluster genes, plus an additional antisense transcript of *hygR* (Figure S5c). These previously not considered promoters created a

FIGURE 7 Impact of talc microparticles on nine major classes of natural products across different actinobacterial families. RiPP-type cinnamycins using *S. albus* pCinCatInt (Lopatniuk et al., 2017), RiPP-type bottromycins using *S. lividans* TK24 DG2-Km-P41hyg + (Horbal et al., 2018), alkaloid-type undecylprodigiosin using *S. lividans* TK24 DG2-Km-P41hyg + (Horbal et al., 2018), angucyclinone-type simocyclinones using *K. sp.* (Bilyk et al., 2016), polyketide-type pamamycins using *S. albus* J1074/R2 (Rebets et al., 2015), polyketide-type alpiniamides using *S. sp.* IB2014/011-12 (Paulus et al., 2018), glycopeptide-type vancomycin using *A. japonicum* DSM 44213 (Stegmann et al., 2014), glycopeptide-type teicoplanin using *A. teichomyceticus* ATCC 31121 (Horbal et al., 2012), nybomycin using *S. albus* subsp. *chlorinus* NRRL B-24108 (Rodriguez Estevez et al., 2018), tetracycline-type oxytetracycline using *S. rimosus* ATCC 10970 (Pethick et al., 2013), tetrahydroisochinoline-type perquinolines using *S. sp.* IB2014/016-6 (Rebets et al., 2019), and anthramycin-type usabamycins using *S. albus* subsp. *chlorinus* NRRL B-24108 (nybomycin) (Rodriguez Estevez et al., 2018). All strains were incubated over 5 days using miniaturized microtiter plate cultures (1 ml) at different talc levels between 0 and 50 g L^{-1}. The natural product levels were determined after solvent extraction using HPLC-ESI-MS and reflect final titers after 5 days. The colored circles given beside strain names indicate the type of producers studied: native (blue circle) and heterologous strains (orange circle). The colored squares denote the underlying control type for cluster expression: native (blue square) and synthetic regulation (orange square). *n* = 3 [Color figure can be viewed at wileyonlinelibrary.com]

complex control architecture and could play a major role in mediating the talc-effect.

4.3 | Microparticles affect submerged culture morphology and accelerate morphological development and aging of *S. lividans* and *S. albus*

The insights into the impact of talc microparticles on morphological development (Figure 4) and the associated cellular program of *S. lividans* (Figures 5, 6, S4, and S6) and the picture recently obtained for the talc effects on the related strain *S. albus* (Kuhl et al., 2020), now allowed to draw a few important conclusions related to morphology and its control in these type of bacteria.

As shown, talc reduced the pellet size of both strains (Figure 3a) (Kuhl et al., 2020), and this response can be expected also in other actinobacteria (Ren et al., 2015), although exceptions cannot be excluded. From the bioengineering viewpoint, smaller pellets appear favorable, as they reduce problems with mass and oxygen transfer limitation, slow growth, and culture heterogeneity (Mehmood et al., 2012; Tamura et al., 1997; van Dissel & van Wezel, 2018; van Dissel et al., 2014).

The strength of the talc-effect was quite different for the two strains. While $10\,g\,L^{-1}$ of the talc material reduced the pellet size of *S. albus* more than six-fold (Kuhl et al., 2020), the same amount of talc did much less to *S. lividans*, as its pellets still maintained 60% of the size of the control culture. The stronger resistance of *S. lividans* might be related to its more dense and compact aggerates, offering less attack points for fragmentation and segregation than the more open and loose structures of *S. albus* (Zacchetti et al., 2018). In addition, differences in cell wall composition, mechanical strength, and hydrophobicity of spores, hyphae, and mycelia could explain the different accessibility of these bacteria to talc-mediated morphology engineering and might be interesting to study further (Driouch, Roth, Dersch, et al., 2010a, 2010b; Driouch et al., 2010; Driouch et al., 2012; Walisko et al., 2012).

Notably, the microparticles accelerated the morphological development of the studied *Streptomyces* in submerged culture. *S. lividans* revealed a premature activation of regulator genes, such as *sigN*, *bldN*, *ssgA*, *ssgB*, and *wblA* (Tables 2 and 3), important control elements of morphology development in *Streptomyces* (Kang et al., 2007; Rebets et al., 2018; Traag & van Wezel, 2008). The same picture of accelerated aging was recently observed for talc-treated *S. albus* (Kuhl et al., 2020), although the microparticles affected the expression of a much higher number of genes in this microbe (56% of all genes) (Kuhl et al., 2020). *S. lividans*, in contrast to *S. albus*, does not sporulate in liquid culture (Daza et al., 1989; Rebets et al., 2018). Differences in morphology control and development on the species level are likely the reason for the observed individual differences. However, the overall response to the microparticle addition

apparently was the same for both strains: accelerated morphology development and aging and it appears likely that other actinobacteria will behave in a similar way.

4.4 | The use of microparticles displays a powerful approach to support natural product research in actinobacteria

As shown, microparticle-based cultures revealed a notably increased performance in producing natural products. First, the addition of talc beneficially increased the formation of 75% of the tested natural products, covering seven important classes with a highly diverse structure: polyketides, glycopeptides, RiPPs, alkaloids, tetracyclines, anthramycin-analogs, and angucyclinone-analogs with different structure (Figures 1 and 7). Stimulating production was observed for molecules of clinical relevance as antibiotics (vancomycin, oxytetracycline, and teicoplanin) (Elsayed et al., 2015; Fung et al., 2012; Liu et al., 2018) for several high-potential candidates presently under development into antibiotics (bottromycin, cinnamycin, pamamycin, and simocyclinone) (Buttner et al., 2017; Kobayashi et al., 2010; Lefèvre et al., 2004; Lopatniuk et al., 2017) and antitumor drugs (undecylprodigiosin and usabamycin) (Sato et al., 2011; Stankovic et al., 2014). Second, the microparticle-approach worked on actinobacteria from different families, including six strains of the most important *Streptomyces* group, plus representatives of the genera *Amycolatopsis*, *Actinoplanes*, and *Kitasatospora*. Third, optimized performance was observed for various strain backgrounds: natural producers, heterologous hosts, and strains expressing the gene cluster of interest under native and under synthetic control. Hereby, one example (teicoplanin) demonstrated that microparticles can even enable formation of a natural product, normally not observed (Figure 7). Fourth, the approach is simple. All what is needed is to add a little bit of talcum powder into the medium. Although the optimum talc level differed between strains and products, a concentration of $10\,g\,L^{-1}$ always revealed a significant effect. Altogether, microparticle-enhanced cultivation provides a valuable concept for natural product research in actinobacteria, complementing efforts to streamline eukaryotic filamentous fungi (Böl et al., 2020; Veiter et al., 2018).

5 | CONCLUSIONS

As shown, talc-supplementation boosted production of seven classes of commercially relevant natural products across strains from different actinobacterial families, including natural as well as heterologous producers. The improvement was up to 100-fold. Obviously, the talc-effect generally accelerated morphological development and aging, inter alia leading to enhanced expression (Kuhl et al., 2020) and re-balanced expression (this study) of the bacterial gene clusters of interest. It is well known that antibiotic production in *Streptomyces* correlates to morphological development (Chater, 1984) and certain natural products are even

part of programmed cell death (PCD) (Tenconi et al., 2018) so that the microparticles obviously trigger a sweet spot towards enhanced performance.

Without doubt, the microparticle concept appears useful to be systematically applied to the field of natural product research, where it offers several striking opportunities. Its successful application at the small scale shows potential for screening efforts to support research on major questions: discovery of novel molecules, activation of silent gene clusters, supply of sufficient amounts for structure elucidation, and exploration of biosynthetic control mechanisms, among others. The applicability to the microliter and microtiter plate scale provides a nice extension to recent developments on miniaturized physiological characterization of *Streptomyces* (Koepff et al., 2017). It appears promising to rescreen some of the libraries of isolates available worldwide, adding a bit of talc (Barka et al., 2016; Landwehr et al., 2016; Silva et al., 2020; Steele et al., 2019). Moreover, given the enormous interest to tailor cellular morphology in actinobacteria for improved performance (Koebsch et al., 2009; van Dissel et al., 2014; van Wezel et al., 2006; Wang et al., 2017; Xu et al., 2008), the microparticle addition seems useful to be tested on the many existing actinobacterial strains, genetically not accessible (Atanasov et al., 2021).

Regarding industrial manufacturing of natural products at large scale, talc could provide a straightforward drop-in solution. It is available in huge amounts, approximately 8 million tons per year according to recent market reviews. The material is cheap, in the range of 10 EUR cents per kg. As an example, supplementation of a $100 \, \text{m}^3$ production process with $10 \, \text{g L}^{-1}$ talc (found effective) would add only costs in the range of 100 EUR. Moreover, co-harvested talc could upgrade fermentation biomass for post-process valorization, given its excellent performance as coating and baking agent in fertilizer formulations (Kaji et al., 2017) and its proven safety and efficacy as feed additive to all animal species (Mallet et al., 2005; Rychen et al., 2018).

Furthermore, it appears interesting to explore the interaction between microparticles and cells in more detail. On the particle side, talc prevented spore agglomeration during the initial culture phase of the fungus *Aspergillus niger*, whereas chemical (nutritional) effects by leached talc minerals played no significant role for the altered morphogenesis (Driouch et al., 2010). Moreover, particle size and shape were found critical. Even a small increase in particle diameter from 6 to 15 µm resulted in a severe loss of the morphology effects, and lamellar shaped talc particles were found more efficient to tailor morphology than round shaped materials (Driouch, 2009). Given the various sizes and shapes of talc, achievable from ball, rod, and autogenous mills, more systematic studies appear feasible. So far not explored but interesting seems the importance of the material softness, as talc is the softest known mineral. Hereby, several other micro materials such as aluminum oxide (Driouch et al., 2010) and titanium silicate oxide (Driouch et al., 2012) await to be tested. On the cellular side, an inspection of the impact of cell wall composition, mechanical strength, and hydrophobicity of spores, hyphae, and mycelia seems relevant, as stated above. Moreover, more research will be needed to clarify the talc-effects in stirred tanks and at large scale, exhibiting different hydrodynamics and mixing regimes (Bliatsiou et al., 2020; Kowalska et al., 2020).

CONFLICT OF INTERESTS

The authors declare that there are no conflict of interests.

AUTHOR CONTRIBUTIONS

Christoph Wittmann designed and supervised the project. Martin Kuhl conducted the cultures and performed substrate and natural product analysis. Christian Rückert and Jörn Kalinowski performed genomics and transcriptomics of *S. lividans*. Martin Kuhl and Lars Gläser performed metabolomics of *S. lividans*. Martin Kuhl and Christoph Wittmann analyzed the data, drew the figures, and wrote the first draft of the manuscript. All authors commented, extended, and improved the manuscript. All authors read and approved the final version of the manuscript.

DATA AVAILABILITY STATEMENT

The data that supports the findings of this study are available in the supplementary material of this article.

ORCID

Christoph Wittmann http://orcid.org/0000-0002-7952-985X

REFERENCES

Ahmed, Y., Rebets, Y., Estevez, M. R., Zapp, J., Myronovskyi, M., & Luzhetskyy, A. (2020). Engineering of *Streptomyces lividans* for heterologous expression of secondary metabolite gene clusters. *Microbial Cell Factories*, 19(1), 5. https://doi.org/10.1186/s12934-020-1277-8

Angert, E. R. (2005). Alternatives to binary fission in bacteria. *Nature Reviews Microbiology*, 3(3), 214–224. https://doi.org/10.1038/nrmicro1096

Arcamone, F., Cassinelli, G., Fantini, G., Grein, A., Orezzi, P., Pol, C., & Spalla, C. (1969). Adriamycin, 14-hydroxydaimomycin, a new antitumor antibiotic from *S. Peucetius* var. *caesius*. *Biotechnology and Bioengineering*, 11(6), 1101–1110. https://doi.org/10.1002/bit.260110607

Atanasov, A. G., Zotchev, S. B., Dirsch, V. M., & Supuran, C. T. (2021). Natural products in drug discovery: Advances and opportunities. *Nature Reviews Drug Discovery*, 20, 1–17.

Barka, E. A., Vatsa, P., Sanchez, L., Gaveau-Vaillant, N., Jacquard, C., Klenk, H.-P., Clément, C., Ouhdouch, Y., & van Wezel, G. P. (2016). Taxonomy, physiology, and natural products of Actinobacteria. *Microbiology and Molecular Biology Reviews*, 80(1), 1–43.

Bayer, vE., Gugel, K., Hägele, K., Hagenmaier, H., Jessipow, S., König, W., & Zähner, H. (1972). Stoffwechselprodukte von mikroorganismen. 98. Mitteilung. Phosphinothricin und phosphinothricyl-alanyl-alanin. *Helvetica Chimica Acta*, *55*(1), 224–239. https://doi.org/10.1002/hlca.19720550126

Bibb, M. J. (2013). Understanding and manipulating antibiotic production in Actinomycetes. *Biochemical Society Transactions*, *41*(6), 1355–1364. https://doi.org/10.1042/BST20130214

Bilyk, O., Brötz, E., Tokovenko, B., Bechthold, A., Paululat, T., & Luzhetskyy, A. (2016). New simocyclinones: Surprising evolutionary and biosynthetic insights. *ACS Chemical Biology*, *11*(1), 241–250.

Bliatsiou, C., Schrinner, K., Waldherr, P., Tesche, S., Böhm, L., Kraume, M., & Krull, R. (2020). Rheological characteristics of filamentous cultivation broths and suitable model fluids. *Biochemical Engineering Journal*, *163*, 107746.

Böl, M., Schrinner, K., Tesche, S., & Krull, R. (2020). Challenges of influencing cellular morphology by morphology engineering techniques and mechanical induced stress on filamentous pellet systems: A critical review. *Engineering in Life Sciences*, *21*, 51–67.

Butterworth, J. H., & Morgan, E. (1968). Isolation of a substance that suppresses feeding in locusts. *Chemical Communications (London)*, (1), 23–24.

Buttner, M. J., Schäfer, M., Lawson, D. M., & Maxwell, A. (2017). Structural insights into simocyclinone as an antibiotic, effector ligand and substrate. *FEMS Microbiology Reviews*, *42*(1):fux055. https://doi.org/10.1093/femsre/fux055

Campbell, W. C., Fisher, M. H., Stapley, E. O., Albers-Schönberg, G., & Jacob, T. A. (1983). Ivermectin: A potent new antiparasitic agent. *Science*, *221*(4613), 823–828. https://doi.org/10.1126/science.6308762

Chater, K. F. (1984). Morphological and physiological differentiation in *Streptomyces*. *Microbial Development*, *16*, 89–115. https://doi.org/10.1101/0.89-115

Chater, K. F., & Losick, R. (1997). Mycelial life style of *Streptomyces coelicolor* A3 (2) and itrs relatives. *Multicellular and interactive Behavior of Bacteria: In Nature, Industry and the Laboratory*, 149–182.

Cragg, G. M., & Newman, D. J. (2013). Natural products: A continuing source of novel drug leads. *Biochimica et Biophysica Acta (BBA)-General Subjects*, *1830*(6), 3670–3695.

Crone, W. J., Vior, N. M., Santos-Aberturas, J., Schmitz, L. G., Leeper, F. J., & Truman, A. W. (2016). Dissecting bottromycin biosynthesis using comparative untargeted metabolomics. *Angewandte Chemie*, *128*(33), 9791–9795.

Daza, A., Martin, J. F., Dominguez, A., & Gil, J. A. (1989). Sporulation of several species of *Streptomyces* in submerged cultures after nutritional downshift. *Microbiology*, *135*(9), 2483–2491.

Demain, A. L. (2006). From natural products discovery to commercialization: a success story. *Journal of Industrial Microbiology and Biotechnology*, *33*(7), 486–495.

Driouch, H. (2009). Morphology engineering of *Aspergillus niger* for improved β-fructofuranosidase roduction. *New Biotechnology*, *25*(25), S212.

Driouch, H., Sommer, B., & Wittmann, C. (2010). Morphology engineering of *Aspergillus niger* for improved enzyme production. *Biotechnology and Bioengineering*, *105*(6), 1058–1068. https://doi.org/10.1002/bit.22614

Driouch, H., Roth, A., Dersch, P., & Wittmann, C. (2010a). Filamentous fungi in good shape: Microparticles for tailor-made fungal morphology and enhanced enzyme production. *Bioengineered Bugs*, *2*(2), 100–104. https://doi.org/10.4161/bbug.2.2.13757

Driouch, H., Roth, A., Dersch, P., & Wittmann, C. (2010b). Optimized bioprocess for production of fructofuranosidase by recombinant *Aspergillus niger*. *Applied Microbiology and Biotechnology*, *87*(6), 2011–2024. https://doi.org/10.1007/s00253-010-2661-9

Driouch, H., Hänsch, R., Wucherpfennig, T., Krull, R., & Wittmann, C. (2012). Improved enzyme production by bio-pellets of *Aspergillus niger*: targeted morphology engineering using titanate microparticles. *Biotechnology and Bioengineering*, *109*(2), 462–471. https://doi.org/10.1002/bit.23313

Droste, J., Rückert, C., Kalinowski, J., Hamed, M. B., Anne, J., Simoens, K., Bernaerts, K., Economou, A., & Busche, T. (2021). Extensive reannotation of the genome of the model Streptomycete *Streptomyces lividans* TK24 based on transcriptome and proteome information. *Frontiers in Microbiology*, *12*, 744.

Elsayed, E. A., Omar, H. G., & El-Enshasy, H. A. (2015). Development of fed-batch cultivation strategy for efficient oxytetracycline production by *Streptomyces rimosus* at semi-industrial scale. *Brazilian Archives of Biology and Technology*, *58*(5), 676–685. https://doi.org/10.1590/s1516-89132015050184

Eyles, T. H., Vior, N. M., & Truman, A. W. (2018). Rapid and robust yeast-mediated pathway refactoring generates multiple new bottromycin-related metabolites. *ACS Synthetic Biology*, *7*(5), 1211–1218.

Fleming, A. (2001). On the antibacterial action of cultures of a penicillium, with special reference to their use in the isolation of *B. influenzae*. *Bulletin of the World Health Organization*, *79*, 780–790.

Franz, L., Kazmaier, U., Truman, A. W., & Koehnke, J. (2021). Bottromycins-biosynthesis, synthesis and activity. *Natural Product Reports*, https://doi.org/10.1039/D0NP00097C

Fung, F. H., Tang, J. C., Hopkins, J. P., Dutton, J. J., Bailey, L. M., & Davison, A. S. (2012). Measurement of teicoplanin by liquid chromatography-tandem mass spectrometry: Development of a novel method. *Annals of Clinical Biochemistry*, *49*(5), 475–481.

Funke, M., Diederichs, S., Kensy, F., Müller, C., & Büchs, J. (2009). The baffled microtiter plate: Increased oxygen transfer and improved online monitoring in small scale fermentations. *Biotechnology and Bioengineering*, *103*(6), 1118–1128.

Gläser, L., Kuhl, M., Jovanovic, S., Fritz, M., Vögeli, B., Erb, T., Becker, J., & Wittmann, C. (2020). A common approach for absolute quantification of short chain CoA thioesters in industrially relevant gram-positive and gram-negative prokaryotic and eukaryotic microbes. *Microbial Cell Factories*, *19*(1), 160.

Hanson, J. R. (2003). *Natural products: The secondary metabolites* (17). Royal Society of Chemistry

Harvey, A. (2000). Strategies for discovering drugs from previously unexplored natural products. *Drug Discovery Today*, *5*(7), 294–300.

Hilker, R., Stadermann, K. B., Schwengers, O., Anisiforov, E., Jaenicke, S., Weisshaar, B., Zimmermann, T., & Goesmann, A. (2016). ReadXplorer 2: Detailed read mapping analysis and visualization from one single source. *Bioinformatics*, *32*(24), 3702–3708.

Horbal, L., Zaburannyy, N., Ostash, B., Shulga, S., & Fedorenko, V. (2012). Manipulating the regulatory genes for teicoplanin production in *Actinoplanes teichomyceticus*. *World Journal of Microbiology and Biotechnology*, *28*(5), 2095–2100.

Horbal, L., Marques, F., Nadmid, S., Mendes, M. V., & Luzhetskyy, A. (2018). Secondary metabolites overproduction through transcriptional gene cluster refactoring. *Metabolic Engineering*, *49*, 299–315. https://doi.org/10.1016/j.ymben.2018.09.010

Horinouchi, S., & Beppu, T. (1984). Production in large quantities of actinorhodin and undecylprodigiosin induced by afsB in *Streptomyces lividans*. *Agricultural and Biological Chemistry*, *48*(8), 2131–2133.

Huo, L., Rachid, S., Stadler, M., Wenzel, S. C., & Müller, R. (2012). Synthetic biotechnology to study and engineer ribosomal bottromycin biosynthesis. *Chemistry & Biology*, *19*(10), 1278–1287.

Kaji, T., Igarashi, S., Fujibayashi, N., & Kobayashi, S. (2017). Solidity reduction effect of granular compound fertilizer (BB fertilizer) by high purity fine powder talc. *Journal of Japanese Soil Fertilizer Science*, *88*(6), 519–526.

Kang, S.-H., Huang, J., Lee, H.-N., Hur, Y.-A., Cohen, S. N., & Kim, E.-S. (2007). Interspecies DNA microarray analysis identifies WblA as a

pleiotropic down-regulator of antibiotic biosynthesis in *Streptomyces. Journal of Bacteriology*, 189(11), 4315–4319.

Kazmaier, U. (2020). The long, long way to bottromycin. *Israel Journal of Chemistry*, https://doi.org/10.1002/ijch.202000068

Kobayashi, Y., Ichioka, M., Hirose, T., Nagai, K., Matsumoto, A., Matsui, H., Hanaki, H., Masuma, R., Takahashi, Y., & Ōmura, S. (2010). Bottromycin derivatives: Efficient chemical modifications of the ester moiety and evaluation of anti-MRSA and anti-VRE activities. *Bioorganic & Medicinal Chemistry Letters*, 20(20), 6116–6120.

Koebsch, I., Overbeck, J., Piepmeyer, S., Meschke, H., & Schrempf, H. (2009). A molecular key for building hyphae aggregates: The role of the newly identified *Streptomyces* protein HyaS. *Microbial Biotechnology*, 2(3), 343–360. https://doi.org/10.1111/j.1751-7915.2009.00093.x

Koepff, J., Keller, M., Tsolis, K. C., Busche, T., Rückert, C., Hamed, M. B., Anne, J., Kalinowski, J., Wiechert, W., Economou, A., & Oldiges, M. (2017). Fast and reliable strain characterization of *Streptomyces lividans* through micro-scale cultivation. *Biotechnology and Bioengineering*, 114(9), 2011–2022.

Kohlstedt, M., Sappa, P. K., Meyer, H., Maass, S., Zaprasis, A., Hoffmann, T., Becker, J., Steil, L., Hecker, M., van Dijl, J. M., Lalk, M., Mader, U., Stulke, J., Bremer, E., Volker, U., & Wittmann, C. (2014). Adaptation of *Bacillus subtilis* carbon core metabolism to simultaneous nutrient limitation and osmotic challenge: A multi-omics perspective. *Environmental Microbiology*, 16(6), 1898–1917. https://doi.org/10.1111/1462-2920.12438

Kowalska, A., Boruta, T., & Bizukojć, M. (2020). Performance of fungal microparticle-enhanced cultivations in stirred tank bioreactors depends on species and number of process stages. *Biochemical Engineering Journal*, 161, 107696.

Kuhl, M., Gläser, L., Rebets, Y., Rückert, C., Sarkar, N., Hartsch, T., Kalinowski, J., Luzhetskyy, A., & Wittmann, C. (2020). Microparticles globally reprogram *Streptomyces albus* toward accelerated morphogenesis, streamlined carbon core metabolism, and enhanced production of the antituberculosis polyketide pamamycin. *Biotechnology and Bioengineering*, 117(112), 3858–3875. https://doi.org/10.1002/bit.27537

Landwehr, W., Wolf, C., & Wink, J. (2016). Actinobacteria and myxobacteria: Two of the most important bacterial resources for novel antibiotics. *How to Overcome the Antibiotic Crisis*, 398, 273–302.

Langmead, B., & Salzberg, S. L. (2012). Fast gapped-read alignment with Bowtie 2. *Nature Methods*, 9(4), 357–359.

Lefèvre, P., Peirs, P., Braibant, M., Fauville-Dufaux, M., Vanhoof, R., Huygen, K., Wang, X.-M., Pogell, B. M., Wang, Y., Fischer, P., Metz, P., & Content, J. (2004). Antimycobacterial activity of synthetic pamamycins. *Journal of Antimicrobial Chemotherapy*, 54(4), 824–827. https://doi.org/10.1093/jac/dkh402

Li, J. W.-H., & Vederas, J. C. (2009). Drug discovery and natural products: End of an era or an endless frontier? *Science*, 325(5937), 161–165.

Liao, Y., Smyth, G. K., & Shi, W. (2014). featureCounts: An efficient general purpose program for assigning sequence reads to genomic features. *Bioinformatics*, 30(7), 923–930.

Liu, M., Yang, Z.-H., & Li, G.-H. (2018). A novel method for the determination of vancomycin in serum by high-performance liquid chromatography-tandem mass spectrometry and its application in patients with diabetic foot infections. *Molecules*, 23(11), 2939.

Lopatniuk, M., Myronovskyi, M., & Luzhetskyy, A. (2017). *Streptomyces albus*: A new cell factory for non-canonical amino acids incorporation into ribosomally synthesized natural products. *ACS Chemical Biology*, 12(9), 2362–2370. https://doi.org/10.1021/acschembio.7b00359

Love, M. I., Huber, W., & Anders, S. (2014). Moderated estimation of fold change and dispersion for RNA-seq data with DESeq. 2. *Genome Biology*, 15(12), 1–21.

Mallet, S., Delord, P., Juin, H., & Lessire, M. (2005). Effect of in feed talc supplementation on broiler performance. *Animal Research*, 54(6), 485–492.

Mehmood, N., Olmos, E., Goergen, J.-L., Blanchard, F., Marchal, P., Klöckner, W., Büchs, J., & Delaunay, S. (2012). Decoupling of oxygen transfer and power dissipation for the study of the production of pristinamycins by *Streptomyces pristinaespiralis* in shaking flasks. *Biochemical Engineering Journal*, 68, 25–33.

Myronovskyi, M., Rosenkränzer, B., Stierhof, M., Petzke, L., Seiser, T., & Luzhetskyy, A. (2020). Identification and heterologous expression of the albucidin gene cluster from the marine strain *Streptomyces Albus* subsp. *Chlorinus* NRRL B-24108. *Microorganisms*, 8(2), 237.

Patridge, E. V., Gareiss, P. C., Kinch, M. S., & Hoyer, D. W. (2015). An analysis of original research contributions toward FDA-approved drugs. *Drug Discovery Today*, 20(10), 1182–1187.

Paulus, C., Rebets, Y., Zapp, J., Rückert, C., Kalinowski, J., & Luzhetskyy, A. (2018). New alpiniamides from *Streptomyces sp.* IB2014/011-12 assembled by an unusual hybrid non-ribosomal peptide synthetase trans-AT polyketide synthase enzyme. *Frontiers in Microbiology*, 9, 1959.

Pethick, F., MacFadyen, A., Tang, Z., Sangal, V., Liu, T.-T., Chu, J., Kosec, G., Petkovic, H., Guo, M., & Kirby, R. (2013). Draft genome sequence of the oxytetracycline-producing bacterium *Streptomyces rimosus* ATCC 10970. *Genome Announcements*, 1(2), e0006313.

Rebets, Y., Brotz, E., Manderscheid, N., Tokovenko, B., Myronovskyi, M., Metz, P., Petzke, L., & Luzhetskyy, A. (2015). Insights into the pamamycin biosynthesis. *Angewandte Chemie*, 54(7), 2280–2284. https://doi.org/10.1002/anie.201408901

Rebets, Y., Tsolis, K. C., Guðmundsdóttir, E. E., Koepff, J., Wawiernia, B., Busche, T., Bleidt, A., Horbal, L., Myronovskyi, M., & Ahmed, Y. (2018). Characterization of sigma factor genes in *Streptomyces lividans* TK24 using a genomic library-based approach for multiple gene deletions. *Frontiers in Microbiology*, 9, 3033.

Rebets, Y., Nadmid, S., Paulus, C., Dahlem, C., Herrmann, J., Hübner, H., Rückert, C., Kiemer, A. K., Gmeiner, P., & Kalinowski, J. (2019). Perquinolines A–C: Unprecedented bacterial tetrahydroisoquinolines involving an intriguing biosynthesis. *Angewandte Chemie International Edition*, 58(37), 12930–12934.

Ren, H., Wang, B., & Zhao, H. (2017). Breaking the silence: New strategies for discovering novel natural products. *Current Opinion in Biotechnology*, 48, 21–27.

Ren, X.-D., Xu, Y.-J., Zeng, X., Chen, X.-S., Tang, L., & Mao, Z.-G. (2015). Microparticle-enhanced production of ε-poly-L-lysine in fed-batch fermentation. *RSC Advances*, 5(100), 82138–82143. https://doi.org/10.1039/C5RA14319E

Rodriguez Estevez, M., Myronovskyi, M., Gummerlich, N., Nadmid, S., & Luzhetskyy, A. (2018). Heterologous expression of the nybomycin gene cluster from the marine strain *Streptomyces albus* subsp. *chlorinus* NRRL B-24108. *Marine Drugs*, 16(11), https://doi.org/10.3390/md16110435

Rychen, G., Aquilina, G., Azimonti, G., Bampidis, V., Bastos, M.dL., Bories, G., Chesson, A., Cocconcelli, P. S., & Flachowsky, G. (2018). EFSA panel on additives. products or substances used in animal feed. Safety and efficacy of natural mixtures of talc (steatite) and chlorite (E 560) as a feed additive for all animal species. *EFSA Journal*, 16(3), e05205.

Sato, S., Iwata, F., Yamada, S., Kawahara, H., & Katayama, M. (2011). Usabamycins A–C: New anthramycin-type analogues from a marine-derived actinomycete. *Bioorganic & Medicinal Chemistry Letters*, 21(23), 7099–7101.

Schneider, C. A., Rasband, W. S., & Eliceiri, K. W. (2012). NIH Image to ImageJ: 25 years of image analysis. *Nature Methods*, 9(7), 671–675. https://doi.org/10.1038/nmeth.2089

Schwechheimer, S. K., Becker, J., Peyriga, L., Portais, J.-C., Sauer, D., Müller, R., Hoff, B., Haefner, S., Schröder, H., & Zelder, O. (2018).

Improved riboflavin production with *Ashbya gossypii* from vegetable oil based on 13C metabolic network analysis with combined labeling analysis by GC/MS, LC/MS, 1D, and 2D NMR. *Metabolic Engineering*, *47*, 357–373.

Ser, H.-L., Law, J. W.-F., Chaiyakunapruk, N., Jacob, S. A., Palanisamy, U. D., Chan, K.-G., Goh, B.-H., & Lee, L.-H. (2016). Fermentation conditions that affect clavulanic acid production in *Streptomyces clavuligerus*: A systematic review. *Frontiers in Microbiology*, *7*, 522.

Sevillano, L., Vijgenboom, E., van Wezel, G. P., Díaz, M., & Santamaría, R. I. (2016). New approaches to achieve high level enzyme production in *Streptomyces lividans*. *Microbial Cell Factories*, *15*(1), 1–10.

Silva, L. J., Crevelin, E. J., Souza, D. T., Lacerda-Júnior, G. V., de Oliveira, V. M., Ruiz, A. L. T. G., Rosa, L. H., Moraes, L. A. B., & Melo, I. S. (2020). Actinobacteria from Antarctica as a source for anticancer discovery. *Scientific Reports*, *10*(1), 1–15.

Stankovic, N., Senerovic, L., Ilic-Tomic, T., Vasiljevic, B., & Nikodinovic-Runic, J. (2014). Properties and applications of undecylprodigiosin and other bacterial prodigiosins. *Applied Microbiology and Biotechnology*, *98*(9), 3841–3858.

Steele, A. D., Teijaro, C. N., Yang, D., & Shen, B. (2019). Leveraging a large microbial strain collection for natural product discovery. *Journal of Biological Chemistry*, *294*(45), 16567–16576.

Stegmann, E., Albersmeier, A., Spohn, M., Gert, H., Weber, T., Wohlleben, W., Kalinowski, J., & Rückert, C. (2014). Complete genome sequence of the actinobacterium *Amycolatopsis japonica* MG417-CF17T (= DSM 44213T) producing (S, S)-N, N′-ethylenediaminedisuccinic acid. *Journal of Biotechnology*, *189*, 46–47.

Takeuchi, S., Hirayama, K., Ueda, K., Sakai, H., & Yonehara, H. (1958). Blasticidin S, a new antibiotic. *The Journal of Antibiotics, Series A*, *11*(1), 1–5.

Tamura, S., Park, Y., Toriyama, M., & Okabe, M. (1997). Change of mycelial morphology in tylosin production by batch culture of Streptomyces fradiae under various shear conditions. *Journal of Fermentation and Bioengineering*, *83*(6), 523–528.

Tang, L., Zhang, Y.-X., & Hutchinson, C. R. (1994). Amino acid catabolism and antibiotic synthesis: Valine is a source of precursors for macrolide biosynthesis in *Streptomyces ambofaciens* and *Streptomyces fradiae*. *Journal of Bacteriology*, *176*(19), 6107–6119.

Tenconi, E., Traxler, M. F., Hoebreck, C., Van Wezel, G. P., & Rigali, S. (2018). Production of prodiginines is part of a programmed cell death process in *Streptomyces coelicolor*. *Frontiers in Microbiology*, *9*, 1742.

Thykaer, J., Nielsen, J., Wohlleben, W., Weber, T., Gutknecht, M., Lantz, A. E., & Stegmann, E. (2010). Increased glycopeptide production after overexpression of shikimate pathway genes being part of the balhimycin biosynthetic gene cluster. *Metabolic Engineering*, *12*(5), 455–461.

Traag, B. A., & van Wezel, G. P. (2008). The SsgA-like proteins in Actinomycetes: Small proteins up to a big task. *Antonie Van Leeuwenhoek*, *94*(1), 85–97. https://doi.org/10.1007/s10482-008-9225-3

van Dissel, D., & van Wezel, G. P. (2018). Morphology-driven downscaling of *Streptomyces lividans* to micro-cultivation. *Antonie Van Leeuwenhoek*, *111*(3), 457–469. https://doi.org/10.1007/s10482-017-0967-7

van Dissel, D., Claessen, D., & van Wezel, G. P. (2014). Morphogenesis of *Streptomyces* in submerged cultures. *Advances in Applied Microbiology*, *89*, 1–45.

van Wezel, G. P., White, J., Hoogvliet, G., & Bibb, M. J. (2000). Application of *redD*, the transcriptional activator gene of the undecylprodigiosin biosynthetic pathway, as a reporter for transcriptional activity in *Streptomyces coelicolor* A3 (2) and *Streptomyces lividans*. *Journal of Molecular Microbiology and Biotechnology*, *2*(4), 551–556.

van Wezel, G. P., Krabben, P., Traag, B. A., Keijser, B. J., Kerste, R., Vijgenboom, E., Heijnen, J. J., & Kraal, B. (2006). Unlocking *Streptomyces spp.* for use as sustainable industrial production platforms by morphological engineering. *Applied and Environmental Microbiology*, *72*(8), 5283–5288. https://doi.org/10.1128/AEM.00808-06

Veiter, L., Rajamanickam, V., & Herwig, C. (2018). The filamentous fungal pellet: Relationship between morphology and productivity. *Applied Microbiology and Biotechnology*, *102*(7), 2997–3006.

Vézina, C., Kudelski, A., & Sehgal, S. (1975). Rapamycin (AY-22, 989), a new antifungal antibiotic. I. Taxonomy of the producing Streptomycete and isolation of the active principle. *The Journal of Antibiotics*, *28*(10), 721–726. https://doi.org/10.7164/antibiotics.28.721

Vior, N. M., Cea-Torrescassana, E., Eyles, T. H., Chandra, G., & Truman, A. W. (2020). Regulation of bottromycin biosynthesis involves an internal transcriptional start site and a cluster-situated modulator. *Frontiers in Microbiology*, *11*, 495.

Waisvisz, J., Van Der Hoeven, M., Van Peppen, J., & Zwennis, W. (1957). Bottromycin. I. A new sulfur-containing antibiotic. *Journal of the American Chemical Society*, *79*(16), 4520–4521.

Walisko, R., Krull, R., Schrader, J., & Wittmann, C. (2012). Microparticle based morphology engineering of filamentous microorganisms for industrial bio-production. *Biotechnology Letters*, *34*(11), 1975–1982. https://doi.org/10.1007/s10529-012-0997-1

Wang, H., Zhao, G., & Ding, X. (2017). Morphology engineering of *Streptomyces coelicolor* M145 by sub-inhibitory concentrations of antibiotics. *Scientific Reports*, *7*(1), 13226. https://doi.org/10.1038/s41598-017-13493-y

Wickham, H., Chang, W., & Wickham, M. H. (2016). Package 'ggplot2'. *Create Elegant Data Visualisations Using the Grammar of Graphics. Version*, *2*(1), 1–189.

Wittmann, C., Hans, M., & Heinzle, E. (2002). In vivo analysis of intracellular amino acid labelings by GC/MS. *Analytical Biochemistry*, *307*(2), 379–382.

Xu, H., Chater, K. F., Deng, Z., & Tao, M. (2008). A cellulose synthase-like protein involved in hyphal tip growth and morphological differentiation in *Streptomyces*. *Journal of Bacteriology*, *190*(14), 4971–4978. https://doi.org/10.1128/JB.01849-07

Zacchetti, B., Smits, P., & Claessen, D. (2018). Dynamics of pellet fragmentation and aggregation in liquid-grown cultures of *Streptomyces lividans*. *Frontiers in Microbiology*, *9*, 943. https://doi.org/10.3389/fmicb.2018.00943

Zmijewski, M. J., Jr., Briggs, B. (1989). Biosynthesis of vancomycin: Identification of TDP-glucose: aglycosyl-vancomycin glucosyltransferase from *Amycolatopsis orientalis*. *FEMS Microbiology Letters*, *59*(1-2), 129–133.

SUPPORTING INFORMATION

Additional Supporting Information may be found online in the supporting information tab for this article.